PHYSICAL REVIEW B **78**, 035437 (2008)

Ultrafast electron dynamics in Pb/Si(111) investigated by two-photon photoemission

Patrick S. Kirchmann and Uwe Bovensiepen*
Fachbereich Physik, Freie Universität Berlin, Arnimallee 14, DE-14195 Berlin-Dahlem, Germany
(Received 13 February 2008; revised manuscript received 3 June 2008; published 21 July 2008)

Ultrafast electron dynamics in Pb/Si(111) quantum well structures have been investigated by femtosecond time-resolved two-photon photoemission spectroscopy. Three unoccupied quantum well states (or subbands) as well as an image potential state are identified and analyzed as a function of Pb thickness. Using 1.9 eV photon energy for optical excitation electron-hole pairs are formed in the Pb film and in the Si substrate. The hot electron population in the quantum well states exhibits a biexponential decay and both decay times increase when the energy difference to the Fermi level is reduced. The slower decay component with decay times of 130 and 900 fs is attributed to delayed filling of the states in the adlayer due to electronic relaxation in the Si(111) substrate. The faster decay (30–140 fs) is caused by electron-electron scattering in the Pb film. At a first glance, the extracted decay times increase toward the Fermi level as predicted by the Fermi-liquid theory. However, by investigation of the quantized electronic structure more detailed insight into scattering among defined subbands has been gained. The rise of the excited electron population in the lowest unoccupied quantum well state is delayed by 70 fs which occurs concomitantly with a decay in the second lowest state. We describe this simultaneous decay and rise in the two adjacent subbands by coupled rate equations and attribute it to intersubband scattering. Thereby, we demonstrate the importance of intersubband decay in low-dimensional metallic systems in addition to intraband scattering processes considered in Fermi-liquid theory and derived descriptions.

DOI: 10.1103/PhysRevB.78.035437 PACS number(s): 73.20.At, 79.60.Dp, 78.47.J−

I. INTRODUCTION

Scattering of excited electrons occurs in metals on femtosecond (fs) time scales due to (i) the large phase space for electron-electron (e-e) scattering and (ii) efficient screening of the hole related to the electron by the underlying elementary excitation of an electron-hole pair. Since in metals the electron-ion interaction is weak the electron-scattering rates Γ can reasonably well be approximated by the free-electron model.[1] This holds in particular for simple metals such as Al, Na, or K where Γ is dominated by e-e scattering, shows a weak momentum dependence, and follows approximately a quadratic energy scaling with respect to the Fermi level E_F, $\Gamma_{e\text{-}e} \sim (E-E_F)^2$, as predicted by Fermi-liquid theory.[2] In principal, this scaling also holds for noble metals such as Cu, Ag, and Au. However, it has been shown by *ab initio* calculations using the *GW* approximation for the self-energy of the excited quasiparticle that the contribution of the *d*-band electrons to screening of the electron-electron interaction leads to an increase in the electron lifetimes $\tau_{e\text{-}e}=\hbar/\Gamma_{e\text{-}e}$ compared to the free-electron-gas description.[2,3] In transition metals the larger number of final states in e-e scattering due to *d* bands close to E_F reduces $\tau_{e\text{-}e}$. In addition, a pronounced dependence on the electron momentum is encountered.[2,4–7]

Experimental access to hole lifetimes is facilitated by photoelectron spectroscopy which measures the hole lifetime through the spectral linewidth.[8] Ballistic electron emission spectroscopy can be employed in combination with a sophisticated theory to analyze electron lifetimes.[5] Time-resolved two-photon photoemission (2PPE) on the other hand monitors the decay of an excited electron population directly in the time domain.[9] By two-time-delayed femtosecond laser pulses hot electrons are first excited into bound intermediate states and subsequently photoemitted into vacuum states (Fig. 1, right). Electron lifetimes have been studied intensively by 2PPE in noble and transition metals[10–17] and a comprehensive understanding has been developed by joined experimental and theoretical efforts for image potential states (IPSs) on noble-metal surfaces (see Refs. 18 and 19 and references therein). Up to now, the electron dynamics in simple metals have not been investigated by 2PPE on a comparable level, albeit individual Cs adatoms adsorbed on single-crystal Cu surfaces have received considerable attention.[20,21] On the other hand, thin-film structures on in-

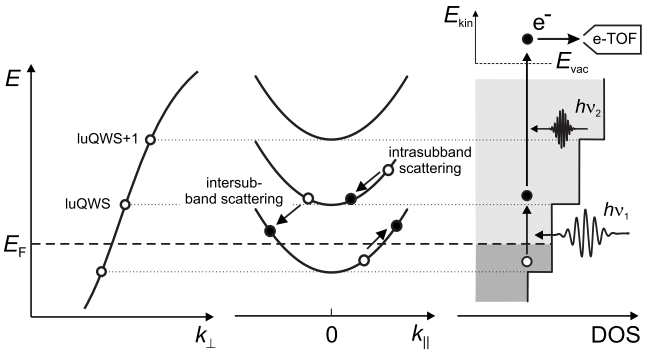

FIG. 1. Left: QWS formation by quantization of the respective bulk valence band in a free-electron-like metal (solid line). Allowed values of $k_\perp$ (○) are determined by the film thickness. Center: idealized dispersion of QWS within the film plane, i.e., along $k_\parallel$. Electron-electron-scattering processes among the subbands are indicated. Right: simplified quantized density of states in a two-dimensional system. The 2PPE process involving the lowest unoccupied QWS (luQWS) is indicated. Excitation of electron-hole pairs occurs by absorption of a visible laser pulse $h\nu_1$. The excited electron is photoemitted by a UV laser pulse $h\nu_2$ and analyzed by an electron time-of-flight spectrometer.

sulating or semiconducting substrates have been shown to be important to limit transport effects that complicate the analysis of electronic lifetimes due to transport effects.[11,15,16] Thus, a promising approach to provide experimental data for simple metals is to prepare thin films and to study the ultrafast electron dynamics as a function of film thickness in order to analyze electronic scattering in the crossover regime between two and three spatial dimensions.

Thin films of *sp* metals such as Al and Pb grown epitaxially on semiconducting substrates, e.g., Si(111),[22–25] present interesting systems to study ultrafast electron dynamics since the electron confinement leads to formation of well-defined occupied and unoccupied quantum well states (QWSs). The respective wave functions are confined to the film and occur at specific electron momenta $k_\perp$ along the film normal which results in a quantization of the free-electron-like band in the direction perpendicular to the film plane, as illustrated in Fig. 1, left. Within the film plane these confined states remain delocalized and the quantization leads to formation of subbands dispersing along parallel electron momentum $k_\parallel$ (see Fig. 1, center and comprehensive reviews by Chiang[26] and Milun *et al.*[27]).

A first study on ultrafast electron dynamics in unoccupied QWS has been reported by Ogawa *et al.*[28] who investigated the system Ag/Fe(001). Albeit this system is well known for its excellent electron confinement to the Ag film from photoelectron spectroscopy under equilibrium conditions,[26] the lifetimes observed by Ogawa *et al.*[28] are below 10 fs for QWS at 1.0–1.6 eV above E_F. Since these are considerably shorter lifetimes than in bulk Ag a nonperfect electron confinement originating from additional decay channels at the interface has been concluded by the authors. A qualitative difference between the Ag/Fe(001) and Pb/Si(111) systems is found in the character of the substrate band gap that facilitates electron confinement. The total band gap in Si requires inelastic-scattering processes if an electron in a QWS is transferred to the substrate. In case of Fe(001) elastic scattering is sufficient as an orientational band is responsible for electron confinement. Considering e-e scattering confined to the adlayer, hot electrons can only decay through intrasubband scattering to the bottom of a particular subband or by intersubband scattering to a lower lying subband. Due to energy and momentum conservation both these processes are accompanied by generation of an electron-hole pair in the vicinity of E_F as depicted in Fig. 1, center.

In this work we report on results of time-resolved two-photon photoemission and investigate the decay of hot electrons in thin Pb films grown epitaxially on Si(111). After a characterization of the unoccupied electronic states in this quantum well system, we identify the electronic relaxation processes in the metallic adlayer as the fastest decaying component (30–140 fs). We observe a delayed rise (~70 fs) of the electron population in the lowest unoccupied QWS (luQWS). This behavior is attributed to intersubband scattering from the next higher lying QWS (luQWS+1). A second slower decay component (130–900 fs) is assigned to relaxation of photoexcited carriers in the Si substrate.

II. EXPERIMENTAL DETAILS

The experimental setup has been described in detail earlier.[16,25,29] In brief, epitaxial Pb films are grown under ultrahigh vacuum (UHV) conditions (base pressure $<1\times10^{-10}$ mbar) in two steps after substrate preparation. First, the Si(111)-7×7 surface reconstruction is formed. Second, the dangling Si bonds are partially saturated by preparation of the Si(111)-$(\sqrt{3}\times\sqrt{3})$-$R30°$-Pb reconstruction.[25] Subsequently, Pb was evaporated from a Knudsen cell and epitaxial Pb(111) films are grown. During the preparation and the 2PPE experiment the temperature was kept at 100 K to avoid island formation and surface diffusion.[30] The evaporation rate of 0.5–1 ML (monolayer)/min was monitored by a quartz-crystal microbalance and cross-checked after deposition by comparison of the observed binding energies of occupied QWS (Ref. 25) with density-functional theory (DFT) calculations from Ref. 31. For characterization of the unoccupied electronic structure, Pb wedges have been grown with a thickness gradient of 5.6 ML/mm.[25]

For bichromatic 2PPE experiments the output of an amplified Ti:sapphire laser system at 300 kHz repetition rate (Coherent RegA 9050) (Ref. 16) is used to drive an optical parametric amplifier (OPA) operating in the visible spectral range. Its tunable signal output $h\nu_1=2.7-1.7$ eV is frequency doubled in a beta barium borate (BBO) crystal and the second harmonic $h\nu_2=5.4-3.4$ eV is generated. Such time-correlated pairs of visible and ultraviolet (UV) femtosecond laser pulses are focused into the UHV chamber and spatially overlapped on the Pb film with typical focus diameters of 100 μm. For 2PPE spectroscopy both pulses overlap in time. For time-resolved 2PPE spectroscopy $h\nu_1$ and $h\nu_2$ are delayed with respect to each other by a controlled variation in the optical path length. Typical fluences for the pump pulse $h\nu_1$ are in the range of 10–30 $\mu J/cm^2$. Additionally, photons of $h\nu=6.2$ eV were generated by frequency quadrupling of the amplifier output to characterize the occupied QWS by one-photon photoemission (1PPE).[25] The binding energy is determined from the kinetic energy E_{kin} of photoelectrons analyzed in an electron time-of-flight spectrometer according to $E-E_F=E_{kin}+\Phi-h\nu$.[32] Here, Φ is the work function and $h\nu$ the photon energy of the probe-laser pulse.

III. RESULTS AND DISCUSSION

We begin with a characterization of the unoccupied electronic structure of Pb/Si(111) by monochromatic 2PPE spectroscopy using UV laser pulses. The photon energy of $h\nu_2=4.05$ eV is chosen to be just below the sample work function[25] which allows us to investigate all bound unoccupied electronic states in Pb/Si(111). 2PPE spectra are shown in Fig. 2 for different film thicknesses ranging from 8 to 19 ML as a function of intermediate-state energy. The spectra exhibit a series of four peaks, which are identified as unoccupied QWS of the Pb $6p_z$ band.

The two peaks at $E-E_F=1.0-1.3$ eV and at $E-E_F=1.4-1.8$ eV for an odd or even number of Pb layers, respectively, clearly disperse toward E_F with increasing film thickness d and thus represent unoccupied QWS confined to the Pb layer. The feature at $E-E_F=0.7$ eV is assigned to the luQWS by comparison to DFT calculations from Ref. 31. To analyze all features in the 2PPE spectra quantitatively a superposition of four Lorentzian peaks and an exponentially

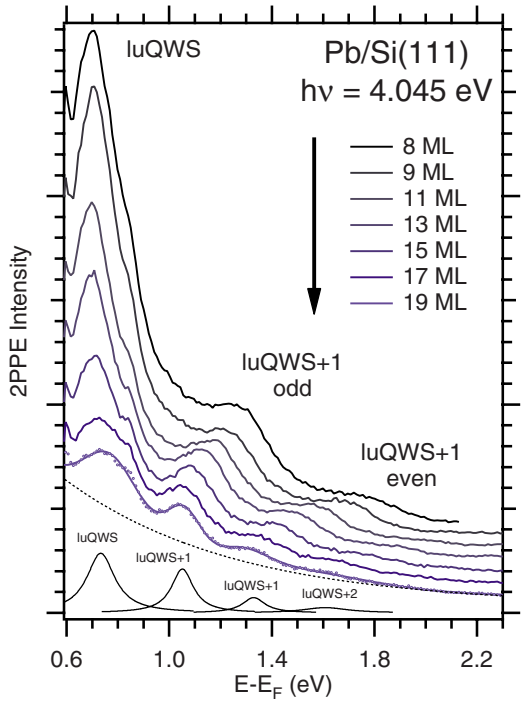

FIG. 2. (Color online) Monochromatic 2PPE spectra recorded with $h\nu_2$=4.05 eV for Pb/Si(111) ultrathin films with varying film thickness. luQWS+1 leads to well resolved peaks which clearly disperse toward E_F with increasing film thickness. luQWS is assigned upon comparison to a DFT calculation (Ref. 31). luQWS +2 is identified by a fit of four Lorentzian peaks and an exponential background which is convoluted with a Gaussian instrument function.

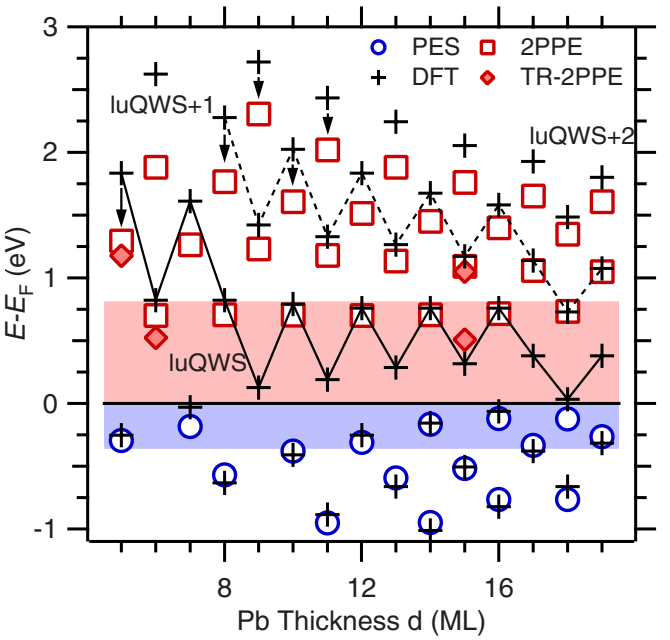

FIG. 3. (Color online) Thickness dependence of QWS energies for occupied and unoccupied states. Open symbols depict energies determined by laser-induced 1PPE (○), by monochromatic (□), and by time-resolved bichromatic (◇) 2PPE. Crosses indicate results from density-functional theory taken from Ref. 31. The solid (dotted) line indicates luQWS (luQWS+1). The shaded area indicates the Si band gap.

falling secondary electron background is fitted to the data which is convoluted with a Gaussian instrument function. The systematic treatment of several subsequent 2PPE spectra at different film thicknesses makes this fitting procedure robust and enables us to identify one more QWS. The intensity of luQWS+2 at $E-E_F$=1.6–2.2 eV is small but can clearly be assigned due to its pronounced dispersion with film thickness. In addition, an IPS at $E-E_F$=3.44 eV (Ref. 33) (not shown, see Fig. 4) is identified and discussed in the context of time-resolved 2PPE experiments.

The energies of unoccupied QWS are extracted from a fit of the monochromatic (□) and time-resolved (◇) 2PPE spectra and depicted in Fig. 3 as a function of layer thickness d in combination with results (+) of a density-functional calculation of a bare Pb slab from Ref. 31. In addition, 1PPE was performed on the identical Pb wedge to characterize the occupied QWS (○), since we have shown in an earlier publication[25] that the results from Ref. 31 and the energies for occupied QWS are in good agreement. The thickness gradient of 5.6 ML/mm of the Pb wedge is rather large compared to the laser spot size of 100 μm and thus photoemission intensity of QWS also occurs at thicknesses where theory does not predict a state. Such cross-talk between subsequent QWSs originates from the finite-thickness resolution due to wedge's slope and the change in the QWS binding energies with Pb thickness gives rise to continuous bands, which disperse toward E_F. Therefore we have chosen an assignment, which is consistent with the theoretically predicted odd-even behavior of the QWS, and only states are depicted in Fig. 3 for the theoretically expected odd or even coverages. For the luQWS peak in Fig. 2, the agreement with the DFT calculations is reasonable. For the higher lying QWS agreement between experiment and calculation is obtained for large d, but with decreasing film thickness significant deviations are encountered. Here, we note that for unoccupied states DFT calculations can lead to deviations because the electronic structure is optimized for the occupied states. On the other hand luQWS+1 is degenerate with the Si conduction band (CB) and the respective interaction is not considered in the calculation. As the deviation between experiment and theory increases for smaller film thickness where interface effects become more pronounced, we consider the interaction of Pb with the Si substrate to be the dominating effect. In the Si band gap such a hybridization is suppressed as the Pb wave function is damped exponentially into Si and the approximation of the Pb film on Si(111) by a freestanding Pb slab apparently holds.

After this characterization of the occupied and unoccupied QWSs we proceed to the time-resolved 2PPE experiments and the ultrafast electron dynamics in Pb/Si(111). For this purpose the UV probe pulse with $h\nu_2$=3.81 eV is time delayed with respect to the visible pump pulses with $h\nu_1$ =1.90 eV and 2PPE spectra are measured as a function of time delay t. As we aim to investigate the electron dynamics within the ultrathin metal film we prepare a 15 ML film where luQWS is situated well in the Si band gap. In this case luQWS+1 is degenerate with Si state as shown in Fig. 3. For

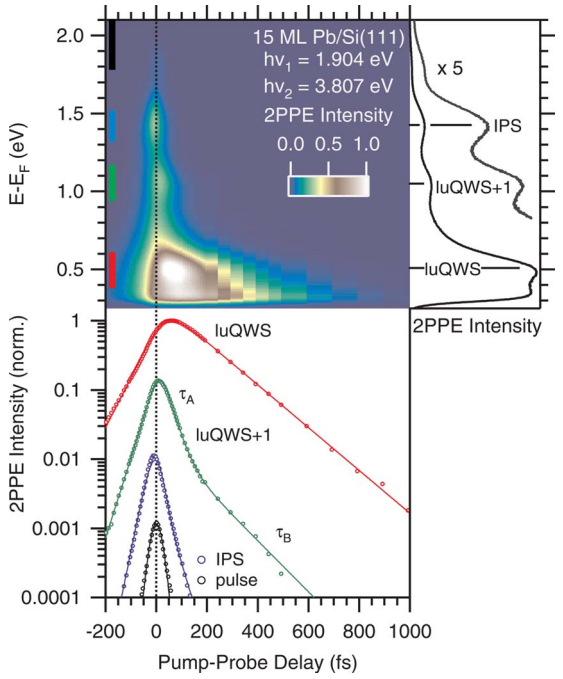

FIG. 4. (Color online) A false color representation of the 2PPE intensity as a function of pump-probe delay and intermediate-state energy $E-E_F$ is given in the center panel. The vertical color bars indicate the energy windows in which the intensity was integrated to monitor the time dependence of the 2PPE intensity. Four spectral features are analyzed (bottom panel), which attributed to luQWS, luQWS+1, an image potential state (IPS), and high-energy electrons. The time dependence of the latter allows a good estimate of the laser-pulse duration. Note that the IPS is excited with the UV pulse $h\nu_2$ and thus its energy is given by $E-E_F=3.33$ eV (Ref. 33), respectively, $E-E_V=-0.76$ eV. Solid lines are fits following a rate equation model (for details see text). These spectral signatures are also seen in the 2PPE spectrum integrated from −65 to 190 fs, given in the right panel.

this thickness the work function is $\Phi=4.09$ eV which allows us to access luQWS and luQWS+1. In the central panel of Fig. 4 the 2PPE intensity is shown as a function of time delay and intermediate-state energy[32] in a false color map. The right part of the figure shows a 2PPE spectrum integrated over t from −65 to 200 fs. The bottom panel depicts the time-dependent 2PPE intensity integrated over different spectral features as indicated by the color bars. In addition to the two QWSs a third state is observed at higher energy. By analysis of the time-dependent intensity we identify this state as the first IPS in front of the Pb(111) surface. Our assignment is based on the fact that the alleged IPS is (i) pumped with the UV light $h\nu_2$, (ii) detected at all thicknesses, (iii) does not disperse with coverage, and (iv) shows a binding energy of −0.76 eV (Ref. 33) with respect to the vacuum level E_V, which agrees with the value expected for the first IPS.[19] Please note the different intermediate energy scales for the IPS, which is pumped by $h\nu_2$.[32] The origin of the IPS is well understood. In brief, the polarization generated in the surface plane by an electron in front of the surface leads to an attractive potential that asymptotically approaches E_V. The image potential gives rise to a series of bound Rydberg-

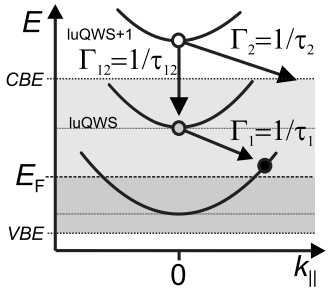

FIG. 5. Visualization of the rate [Eqs. (1) and (2)]. Γ_1 and Γ_2 quantify the depopulation rates of luQWS and luQWS+1 via scattering to unoccupied states. Γ_{12} accounts for the intrasubband scattering luQWS+1 → luQWS.

type series of IPS converging toward E_V. The IPSs are localized in front of the metal surface while being delocalized parallel to the surface plane.[18,19] However, since the origin of the IPS and their dynamics are well understood we will focus on the electron relaxation in the unoccupied QWS in the following.

The bottom panel of Fig. 4 shows cross-correlation (XC) traces which have been integrated over the energy regions indicated by the color bars on the left. The laser-pulse duration is inferred from the XC trace of the hot-electron distribution[29] for $E-E_F>1.8$ eV to be 34(4) fs. The peak maximum of the IPS occurs at formally negative delays (−8 fs) which indicates that the IPS population is build up by the UV pulse $h\nu_2$ and probed by the visible pulse $h\nu_1$.[29,32] Modeling of the XC trace of the IPS by convolution of the laser-pulse's temporal profile and a single exponential decay results in an IPS decay time $\tau=\hbar/\Gamma=24(5)$ fs. This decay constant is of the same order as, e.g., in Cu(111) (Ref. 19) and corroborates the assignment as IPS.

In contrast, the XC traces of luQWS and luQWS+1 show a complex behavior, which requires more than one decay channel as explanation. The electron decay in luQWS is characterized by a delayed rise of the intermediate-state population which leads to a broad peak maximum extending from 30 to 85 fs, while luQWS+1 lacks a delayed rise and presents a biexponential decay. To describe both QWSs consistently we use a rate equation model which takes intersubband scattering from luQWS+1 to luQWS into account,

$$\dot{n}_1(t) = -\Gamma_1 n_1(t) + \Gamma_{12} n_2(t), \tag{1}$$

$$\dot{n}_2(t) = -(\Gamma_{12} + \Gamma_2) n_2(t). \tag{2}$$

These two coupled differential equations describe the transient population $n_1(t)$ and $n_2(t)$ of luQWS and luQWS+1, respectively. Γ_1 accounts for the decay of the excited electron population of luQWS to, e.g., unoccupied states of the metal film near E_F, as sketched in Fig. 5. Γ_{12} describes the delayed filling of luQWS due to intersubband scattering from luQWS+1. Γ_2 summarizes all decay channels of luQWS+1, which are not associated with the intersubband transition luQWS+1 → luQWS. These decay channels may involve scattering to unoccupied states of the Si substrate as well as intersubband scattering to unoccupied states at $k_{\|}$

$\neq 0$ within the metal film. The coupled rate equations are solved analytically to model the population dynamics of luQWS,

$$n_1(t) = \underbrace{n_1^{(0)} e^{-\Gamma_1 t}}_{\text{population decay}} + \underbrace{n_2^{(0)} C(e^{-\Gamma_1 t} - e^{-\Gamma_2' t})}_{\text{delayed population rise}}, \tag{3}$$

$$n_2(t) = n_2^{(0)} e^{-\Gamma_2' t}, \tag{4}$$

with

$$\Gamma_2' = \Gamma_{12} + \Gamma_2 \text{ and } C = \frac{\Gamma_{12}}{\Gamma_2' - \Gamma_1}. \tag{5}$$

The total decay rate, which is directly observed in luQWS+1, is defined as Γ_2'. The case $\Gamma_2' > \Gamma_1$ results in $C > 0$ and Eq. (3) describes a delayed population build up in luQWS and subsequent decay at a rate Γ_1. Thus the coupled rate equation model connects the decay rate Γ_2' observed in the initial decay of luQWS+1 with the population build up in luQWS.

For luQWS the fit of Eq. (3), which is convoluted with the laser-pulse shape, results in $\tau_1 = \hbar/\Gamma_1 = 142(5)$ fs for the decay and a characteristic rise time $\tau_{12} = 54(5)$ fs, which gives an excellent description of the data, as shown in Fig. 4. Fitting of $n_1(t)$ allows us moreover to determine $\tau_2 = 103(10)$ fs [see Eq. (3)]. Turning to luQWS+1, we analyze the population decay by a biexponential decay resulting in a fast decay time of $\tau_A = 30(5)$ fs and a slow one of $\tau_B = 135(10)$ fs.

As a test of our rate equation model the experimentally determined decay time τ_A of luQWS+1 is compared with the total decay time τ_2' calculated within the rate equation model,

$$\tau_2' = \frac{\tau_{12}\tau_2}{\tau_{12} + \tau_2}. \tag{6}$$

For a consistent description of the decay in luQWS as well as luQWS+1, the calculated total decay time τ_2' of luQWS+1 is expected to be identical to the decay time τ_A as observed in the experiment. Within errors bars the calculated value of $\tau_2' = 35(10)$ fs indeed matches the experimentally determined decay time $\tau_A = 30(5)$ fs. Thus we explain the population buildup in luQWS on a time scale τ_{12} and the simultaneous decay of luQWS+1 with $\tau_2' = \tau_A$ by intersubband scattering from luQWS+1 to luQWS.

Before we analyze the slow decay component, we briefly compare the fast decay times attributed to the decay within the metal film with Fermi-liquid theory. We follow Ref. 1 and employ the electron density for bulk Pb of 1.3×10^{29} m^{-3} calculated from 16 valence electrons per unit cell and the Pb lattice constant of 4.95 Å.[34] In general, the observed lifetimes increase toward E_F. The lifetime $\tau_1 = 142(5)$ fs of luQWS matches the value estimated from Fermi-liquid theory of 126 fs reasonably, while for luQWS +1 the theoretical value coincides with the experimental value of $\tau_A = 30(5)$ fs. Thus, Fermi-liquid theory describes the main trend reasonably in agreement with a recent scanning tunneling spectroscopy study on different quantum well systems.[35] Whether the encountered deviation originates from deficiencies of the Fermi-liquid description or from the electron density remains open at this stage.

At this point we would like to remind the reader on the electron lifetimes analyzed by time-resolved 2PPE for unoccupied QWS in Ag/Fe(001) (Ref. 28) which were smaller than 10 fs. The lifetimes we have determined for Pb/Si(111) in a comparable energy interval above E_F are considerably larger than this value. Since Ag and Pb both exhibit *sp* bands in the relevant energy range, we conclude that the substrate or the interface is responsible for these differences in the lifetimes. Generally speaking, we could illustrate nicely that an orientational band gap as in Fe(001) confines electrons to a considerably weaker degree than a total band gap. Elastic scattering from the adlayer to the substrate, which is easily facilitated at the interface due to the break of symmetry and defects arising from lattice mismatch, appears to be the decisive process that limits the residence time of hot electrons in QWS on substrates with orientational band gaps. This finding suggests more systematic studies comparing QWS from the same material on different substrates. Our current study would be complemented nicely by a time-resolved investigation of electron decay in Pb/Cu(111).

In the following we draw the attention to the decay of luQWS+1 at later delays ($t > 200$ fs), which is not analyzed by our rate equation model and is treated separately by an additional exponential decay resulting in $\tau_B = 135(10)$ fs. The biexponential decay of luQWS+1 indicates scattering from higher lying states or states at equal energy, which are significantly longer lived than luQWS+1. These states could be localized either in the Pb film or in the substrate. The pump-photon energy $h\nu_1$ is not sufficient to populate any higher lying states in the film, such as luQWS+2 or any IPS by one-photon processes. Thus, we attribute the decay process described by τ_B to scattering of photoexcited electrons of the Si substrate to the unoccupied QWS in the metal film.

To understand the τ_B component better, we investigated different film thicknesses. Films with few ML thicknesses were prepared. In Fig. 6 XC traces of luQWS at $E-E_F = 1.07$ eV (□) are shown for a 5 ML film and at $E-E_F = 0.53$ eV (○) for 6 ML (cf. Fig. 3). In both cases, a second component τ_B has also been observed in luQWS, which was not found for 15 ML. We find decay times of $\tau_B = 130(10)$ fs for 5 ML and a significantly longer 0.9(1) ps for 6 ML which will be discussed below.

This brings up the question of the photogenerated carrier density in Si under the employed excitation conditions with typical fluences of 10–30 μJ/cm^2. Since we employ pump pulses at 1.9 eV photon energy, indirect transitions and two-photon absorption in Si (Ref. 36) are responsible for the absorption as indicated in the inset of Fig. 6. An experimental analysis of the carrier density would require a systematic temperature and fluence dependence, which is out of the scope of the present paper. Nevertheless, a comparison with earlier studies at similar photon energy and one order larger fluence[37,38] suggests that sizable densities are generated. Note that indeed the population attributed to scattering from Si is considerably smaller than the photogenerated population in the lead film (Fig. 6).

To explain the pronounced energy dependence of τ_B that is encountered for 5 and 6 ML films, we consider scattering

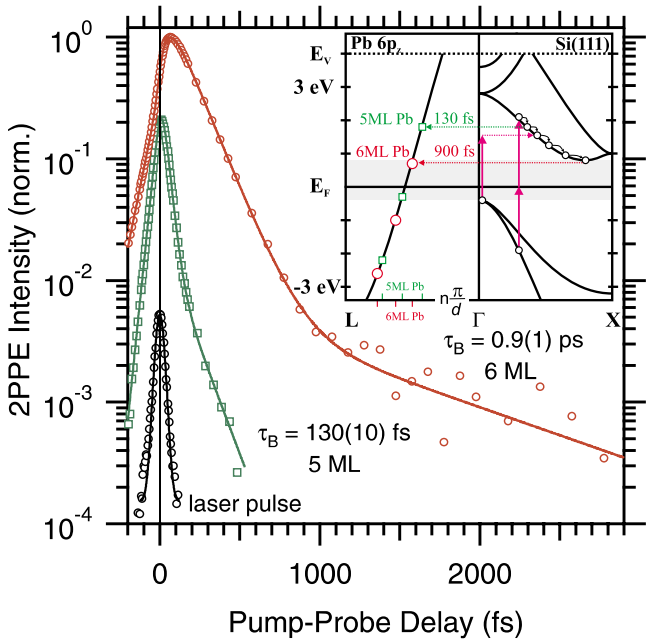

FIG. 6. (Color online) XC traces of luQWS for 5 (○) and 6 (□) ML films, which both exhibit a biexponential decay. The decay component τ_B at later delays is assigned to scattering of photoexcited electrons of the Si substrate to the unoccupied QWS. The inset shows the quantized dispersion of the Pb $6p_z$ QWS along $k_\perp$ and the indirect Si band gap along Γ-X. A possible mechanism explaining the different time scales analyzed for τ_B is depicted.

from the bulk Si CB into the Pb film. We do not take additional relaxation processes in the Pb film into account because in case of 5 ML no higher lying QWS can be populated by the pump pulse, but such excitations do occur in the substrate. Hot electrons in Si relax in a cascade of electrons via phonon-mediated intraband scattering toward the band bottom (see inset of Fig. 6). In bulk Si the energy relaxation time is found to be ~250 fs (Refs. 36 and 39) in the low excitation regime and increases for high excitation densities.[36] The relaxation time on the Si(100) surface is reported to be larger.[40–42] Subsequent energy relaxation at the Si surface proceeds via formation of surface excitons in the Si band gap on a time scale of 5 ps.[40,41] Thus the specific binding energies of luQWS at different thicknesses with respect to the Si CB can be considered to explain the two-time scales observed for τ_B. In case of 5 ML luQWS is degenerate with the Si CB. The relaxation of hot electrons through intraband decay on a few 100 fs time scales in Si is monitored indirectly by means of electrons that scatter quasielastically into the luQWS located in Pb. This serves as a reasonable scenario to explain τ_B of about 130 fs for luQWS at 5 ML and luQWS+1 at 15 ML. In contrast, for 6 ML luQWS resides in the Si band gap. Electrons scattered into luQWS might originate from electrons near the CB minimum in Si, which exhibit a significantly longer lifetime, scatter into the Pb adlayer, and might serve as an explanation for τ_B =900 fs encountered for the 6 ML film. On the basis of these data it cannot be decided unambiguously whether the decay in Si or the scattering to the Pb film is the step that determines τ_B. However, as the intraband decay in the Si CB is mediated by electron-phonon scattering it is rather likely that the 900 fs time scale observed for 6 ML is determined by the decay in Si. Moreover, this time scale agrees with earlier reports reasonably well.[40,42] One could expect that the long lifetimes at the Si CB bottom leads to an even slower decay. However, the presence of the metal facilitates energy gain of the excited electrons by their transfer to the metal film where they can decay to the Fermi level. Thereby, exciton formation in the region near the interface is quenched. We expect further insight from future systematic thickness- and angle-dependent studies.[43]

IV. SUMMARY

The unoccupied electronic structure and ultrafast electron dynamics in unoccupied quantum well states in ultrathin Pb films on Si(111) have been investigated by femtosecond-time-resolved 2PPE. We identify up to three quantum well states above E_F and their dispersion with film thickness. The respective binding energies are in agreement with density-functional calculations of a freestanding Pb film for large thicknesses (~20 ML). At lower thickness systematic deviations occur, most likely due to interaction with the Si substrate. The energy dependence of the decay times in the two QWSs above E_F agrees qualitatively with Fermi-liquid theory. To describe the observed transient population quantitatively it is necessary to account for the quantization of the electronic system. By analysis of the simultaneous population decay and buildup in the two adjacent subbands, we identify intersubband scattering from the second QWS into the first QWS above E_F. Additional decay processes observed on longer time scales with decay times of 130 and 900 fs are attributed to the decay of hot carriers in the Si substrate which are probed in 2PPE because hot electrons scatter from Si into the Pb film. Our analysis demonstrates that the quantization has to be considered explicitly for a description of electron dynamics in the QW subbands. Future angle-resolved investigations[43] are expected to lead to a more comprehensive analysis of intrasubband and intersubband scattering processes. Thereby the influence of (i) the quantization in the two-dimensional structure and (ii) of the Si substrate on electron-electron-scattering rates might be analyzed directly in the time domain.

ACKNOWLEDGMENTS

The authors acknowledge fruitful discussions with and continuous support by M. Wolf. This work has been funded by the Deutsche Forschungsgemeinschaft through BO 1823/2. P.S.K. gratefully acknowledges support by the International Max-Planck Research School "Complex Surfaces in Material Science."

*uwe.bovensiepen@physik.fu-berlin.de; www.physik.fu-berlin.de/~bovensie

[1] D. Pines and P. Nozieres, *The Theory of Quantum Liquids* (Benjamin, New York, 1966).
[2] E. V. Chulkov, A. G. Borisov, J. P. Gauyacq, D. Sánchez-Portal, V. M. Silkin, V. P. Zhukov, and P. M. Echenique, Chem. Rev. (Washington, D.C.) **106**, 4160 (2006).
[3] I. Campillo, J. M. Pitarke, A. Rubio, E. Zarate, and P. M. Echenique, Phys. Rev. Lett. **83**, 2230 (1999).
[4] R. Knorren, K. H. Bennemann, R. Burgermeister, and M. Aeschlimann, Phys. Rev. B **61**, 9427 (2000).
[5] F. Ladstädter, Pilar F. de Pablos, U. Hohenester, P. Puschnig, C. Ambrosch-Draxl, Pedro L. de Andrés, F. J. García-Vidal, and F. Flores, Phys. Rev. B **68**, 085107 (2003).
[6] V. P. Zhukov, E. V. Chulkov, and P. M. Echenique, Phys. Rev. B **72**, 155109 (2005).
[7] A. Mönnich, J. Lange, M. Bauer, M. Aeschlimann, I. A. Nechaev, V. P. Zhukov, P. M. Echenique, and E. V. Chulkov, Phys. Rev. B **74**, 035102 (2006).
[8] A. Gerlach, K. Berge, A. Goldmann, I. Campillo, A. Rubio, J. M. Pitarke, and P. M. Echenique, Phys. Rev. B **64**, 085423 (2001).
[9] H. Petek and S. Ogawa, Prog. Surf. Sci. **56**, 239 (1997).
[10] C. A. Schmuttenmaer, M. Aeschlimann, H. E. Elsayed-Ali, R. J. D. Miller, D. A. Mantell, J. Cao, and Y. Gao, Phys. Rev. B **50**, 8957 (1994).
[11] E. Knoesel, A. Hotzel, and M. Wolf, Phys. Rev. B **57**, 12812 (1998).
[12] H. Petek, A. P. Heberle, W. Nessler, H. Nagano, S. Kubota, S. Matsunami, N. Moriya, and S. Ogawa, Phys. Rev. Lett. **79**, 4649 (1997).
[13] H. Petek, H. Nagano, and S. Ogawa, Phys. Rev. Lett. **83**, 832 (1999).
[14] M. Merschdorf, C. Kennerknecht, and W. Pfeiffer, Phys. Rev. B **70**, 193401 (2004).
[15] M. Aeschlimann, M. Bauer, S. Pawlik, R. Knorren, G. Bouzerar, and K. H. Bennemann, Appl. Phys. A: Mater. Sci. Process. **71**, 485 (2000).
[16] M. Lisowski, P. A. Loukakos, U. Bovensiepen, and M. Wolf, Appl. Phys. A: Mater. Sci. Process. **79**, 739 (2004).
[17] J. Cao, Y. Gao, H. E. Elsayed-Ali, R. J. D. Miller, and D. A. Mantell, Phys. Rev. B **58**, 10948 (1998).
[18] M. Weinelt, J. Phys.: Condens. Matter **14**, R1099 (2002).
[19] P. M. Echenique, R. Berndt, E. V. Chulkov, T. Fauster, A. Goldmann, and U. Höfer, Surf. Sci. Rep. **52**, 219 (2004).
[20] M. Bauer, S. Pawlik, and M. Aeschlimann, Phys. Rev. B **60**, 5016 (1999).
[21] H. Petek, M. J. Weida, H. Nagamo, and S. Ogawa, Science **288**, 1402 (2000).
[22] L. Aballe, C. Rogero, P. Kratzer, S. Gokhale, and K. Horn, Phys. Rev. Lett. **87**, 156801 (2001).
[23] M. H. Upton, C. M. Wei, M. Y. Chou, T. Miller, and T. C. Chiang, Phys. Rev. Lett. **93**, 026802 (2004).
[24] J. H. Dil, J. W. Kim, T. Kampen, K. Horn, and A. R. H. F. Ettema, Phys. Rev. B **73**, 161308(R) (2006).
[25] P. S. Kirchmann, M. Wolf, J. H. Dil, K. Horn, and U. Bovensiepen, Phys. Rev. B **76**, 075406 (2007).
[26] T.-C. Chiang, Surf. Sci. Rep. **39**, 181 (2000).
[27] M. Milun, P. Pervan, and D. Woodruff, Rep. Prog. Phys. **65**, 99 (2002).
[28] S. Ogawa, H. Nagano, and H. Petek, Phys. Rev. Lett. **88**, 116801 (2002).
[29] P. S. Kirchmann, P. A. Loukakos, U. Bovensiepen, and M. Wolf, New J. Phys. **7**, 113 (2005).
[30] M. Hupalo, S. Kremmer, V. Yeh, L. Berbil-Bautista, E. Abram, and M. C. Tringides, Surf. Sci. **493**, 526 (2001).
[31] C. M. Wei and M. Y. Chou, Phys. Rev. B **66**, 233408 (2002).
[32] Determination of the intermediate-state energy scale $E-E_F$ requires knowledge by which pulse the electron is photoemitted. This becomes clear after performing time-resolved experiments because hot electrons decay with increasing delay. In the present setup $h\nu_2$ is delayed with respect to $h\nu_1$. Electrons decaying toward positive (negative) delays are excited by $h\nu_1(h\nu_2)$ and photoemitted by $h\nu_2(h\nu_1)$. Thus the intermediate energy scale for the QWS and IPS differs by $(h\nu_2-h\nu_1)$.
[33] The absolute value of the work function is somewhat different for each wafer prepared, which we attribute to different pinning positions of E_F. Since the IPSs are pinned to E_V the fluctuations of the work function alter the binding energy of the IPS with respect to E_F.
[34] C. Kittel, *Introduction to Solid State Physics* (Wiley, London, 2004).
[35] D. Wegner, A. Bauer, and G. Kaindl, Phys. Rev. Lett. **94**, 126804 (2005).
[36] T. Sjodin, H. Petek, and H.-L. Dai, Phys. Rev. Lett. **81**, 5664 (1998).
[37] J. R. Goldman and J. A. Prybyla, Phys. Rev. Lett. **72**, 1364 (1994).
[38] S. Jeong, H. Zacharias, and J. Bokor, Phys. Rev. B **54**, R17300 (1996).
[39] A. J. Sabbah and D. M. Riffe, Phys. Rev. B **66**, 165217 (2002).
[40] M. Weinelt, M. Kutschera, T. Fauster, and M. Rohlfing, Phys. Rev. Lett. **92**, 126801 (2004).
[41] M. Weinelt, M. Kutschera, R. Schmidt, C. Orth, T. Fauster, and M. Rohlfing, Appl. Phys. A: Mater. Sci. Process. **80**, 995 (2005).
[42] C. Voelkmann, M. Reichelt, T. Meier, S. W. Koch, and U. Höfer, Phys. Rev. Lett. **92**, 127405 (2004).
[43] P. Kirchmann, L. Rettig, D. Nandi, U. Lipowski, M. Wolf, and U. Bovensiepen, Appl. Phys. A: Mater. Sci. Process. **91**, 211 (2008).